European Journal of Neuroscience, Vol. 24, pp. 2749–2757, 2006 doi:10.1111/j.1460-9568.2006.05176.x

Second-by-second measurement of acetylcholine release in prefrontal cortex

John P. Bruno,[1] Clelland Gash,[1] Brad Martin,[1] Amy Zmarowski,[1] Francois Pomerleau,[2] Jason Burmeister,[2] Peter Huettl[2] and Greg A. Gerhardt[2]
[1]Departments of Psychology and Neuroscience, 57 Psychology Building, The Ohio State University, Columbus, OH 43210, USA
[2]Department of Anatomy and Neurobiology, Center for Sensor Technology, University of Kentucky Medical Center, Lexington, KY, USA

Keywords: acetylcholine, prefrontal cortex, nicotine, voltammetry, rat

Abstract

Microdialysis has been widely used to measure acetylcholine (ACh) release *in vivo* and has provided important insights into the regulation of cholinergic transmission. However, microdialysis can be constrained by limited spatial and temporal resolution. The present experiments utilize a microelectrode array (MEA) to rapidly measure ACh release and clearance in anaesthetized rats. The array electrochemically detects, on a second-by-second basis, changes in current selectively produced by the hydrolysis of ACh to choline (Ch) and the subsequent oxidation of choline and hydrogen peroxidase (H_2O_2) at the electrode surface. *In vitro* calibration of the microelectrode revealed linear responses to ACh ($R^2 = 0.9998$), limit of detection of 0.08 μM, and signal-to-noise ratio of 3.0. The electrode was unresponsive to ascorbic acid (AA), dopamine (DA), or norepinephrine (NE) interferents. *In vivo* experiments were conducted in prefrontal cortex (PFC) of anaesthetized rats. Pressure ejections of ACh (10 mM; 40 nL) through an adjoining micropipette produced a rapid rise in current, reaching maximum amplitude in ~1.0 s and cleared by 80% within 4–11 s. Endogenously released ACh, following local depolarization with KCl (70 mM; 40, 160 nL), was detected at values as low as 0.05 μM. These signals were volume-dependent and cleared within 4–12 s. Finally, nicotine (1.0 mM, 80 nL) stimulated ACh signals. Nicotine-induced signals reflected the hydrolysis of ACh by endogenous acetylcholinesterase (AChE) as inhibition of the enzyme following perfusion with neostigmine (10 μM) attenuated the signal (40–94%). Collectively, these data validate a novel method for rapidly measuring cholinergic transmission *in vivo* with a spatial and temporal resolution that far exceeds conventional microdialysis.

Introduction

Corticopetal cholinergic projections from the basal forebrain innervate all areas and layers of the cortical mantle (Mechawar *et al*., 2000) and this diffuse pattern of innervation is consistent with cholinergic afferents' role in the gating of cortical information processing such as the regulation of sleep–wakefulness cycles (Szymusiak, 1995; Jones, 2005) and attentional processing (Everitt & Robbins, 1997; Sarter & Bruno, 1997; Passetti *et al*., 2000; Dalley *et al*., 2001, 2004; Sarter *et al*., 2003, 2005).

Over the past two decades, the *in vivo* measurement of cholinergic transmission has been best studied using the technique of microdialysis. The quantification of acetylcholine (ACh) efflux has revealed the effects of psychoactive and therapeutic drugs on cholinergic transmission (Ichikawa *et al*., 2002; Nelson *et al*., 2000, 2002; Gobert *et al*., 2003; Millan *et al*., 2004) as well as the relationship between complex cognitive behaviours and cortical ACh release (Himmelheber *et al*., 2000; Passetti *et al*., 2000; Dalley *et al*., 2001; Arnold *et al*., 2002; Kozak *et al*., 2006).

While the use of microdialysis methods for the assessment of ACh release has evolved substantially over the past two decades (see Bruno *et al*., 1999; Day *et al*., 2001), the limited spatial and temporal resolution of the technique can constrain potential research questions on cholinergic transmission. With regard to spatial resolution, the sampling radius of the typical microdialysis probe is difficult to precisely quantify, however, estimates suggest a zone as large as one to several millimeters, depending upon the nature of the analyte (Westerink & DeVries, 2001). Moreover, most commercial microdialysis probes are relatively large (i.e. 250–400 μm o.d.). Thus, attempts to study small brain regions or to functionally differentiate contiguous areas have been thwarted by the size of the microdialysis probes and the extended sampling zone. As recent studies have suggested a functional differentiation among regions of the frontal cortex (Hedou *et al*., 2000; Zaborszky, 2002; Golmayo *et al*., 2003; Dalley *et al*., 2004), it is important to determine whether behavioural tasks that selectively tax different cognitive constructs will differentially activate cholinergic inputs to these frontal regions.

At the level of temporal resolution, the analytical methods (e.g. HPLC) have evolved over the past two decades, enhancing the limits of detection and allowing, in some cases, the measurement of basal ACh without the use of an acetylcholinesterase inhibitor (see Bruno *et al*., 1999; Day *et al*., 2001; Ichikawa *et al*., 2002). Even with these improvements the shortest collection intervals typically reported are 6–8 min (Arnold *et al*., 2002; Kozak *et al*., 2006). The use of capillary electrophoresis methods, used in the analysis of other neurotransmitters (Kennedy *et al*., 2002) may reduce these collection intervals even further. However, the time required to harvest sufficient ACh for conventional detection still limits collection intervals to the range of minutes. Several laboratories have reported activation of the cortical

Correspondence: Dr John P. Bruno, as above.
E-mail:bruno.1@osu.edu

Received 22 July 2006, revised 31 August 2006, accepted 12 September 2006

cholinergic system during performance of behavioural tasks designed to explicitly tax attentional processing (Himmelheber *et al*., 2000; Passetti *et al*., 2000; Dalley *et al*., 2001; Arnold *et al*., 2002; Kozak *et al*., 2006). However, the temporal mismatch between task events and dialysis collection intervals has made it difficult to relate specific elements of the task or the animals' responses to changes in ACh release particularly as these behavioural microdialysis experiments have task parameters and responses collapsed across a single microdialysis collection interval.

In vivo voltammetry offers significant improvements over microdialysis in both spatial and temporal resolution. Traditionally, voltammetric techniques have been limited to compounds that are inherently electroactive such as the monoaminergic transmitters. Historically, this has precluded the use of *in vivo* voltammetry to study ACh or the amino acid transmitters (i.e. glutamate, GABA). Recently, we (Burmeister *et al*., 2002, 2003, 2006; Parikh *et al*., 2004; Bruno *et al*., 2006a, b) and others (Garguilo & Michael, 1996; Lowry *et al*., 1998; Cui *et al*., 2001; Mitchell, 2004; Parikh & Sarter, 2006) have reported the development of enzyme-based microelectrodes that convert nonelectroactive molecules into electroactive substances. The nonelectroactive analyte is converted, via a surface-bound enzyme (i.e. oxidase), to hydrogen peroxide (H_2O_2), which is then oxidized and the resulting current is measured. Several studies have focused on the use of this methodology for studying release from cholinergic (Burmeister *et al*., 2002, 2003, 2006; Parikh *et al*., 2004, 2006; Bruno *et al*., 2006a, b) and glutamatergic (Burmeister *et al*., 2002; Pomerleau *et al*., 2003; Day *et al*., 2006) terminal regions.

Our previous work using the enzyme-based microelectrode to study cholinergic transmission focused on a sensor designed to detect changes in extracellular choline as a marker of ACh release (Burmeister *et al*., 2002; Parikh *et al*., 2004). Results from these and other studies (Cui *et al*., 2001; Mitchell, 2004; Parikh & Sarter, 2006) verify that under certain conditions, changes in choline over extremely short time epochs (i.e. 1–10 s) can provide a valid index of ACh release.

There are, however, potential limitations to the use of choline (Ch) levels as a marker for ACh release. Choline is both a precursor for ACh and a product of its degradation (Klein *et al*., 1991; Klein, 2000). Moreover, choline is transported from plasma to extracellular fluid and imported into cells for functions other than neurotransmission, such as membrane formation (Araki & Wurtman, 1998). Thus, a significant component of the basal Ch signal is not due to neuronal release of ACh (Parikh *et al*., 2004). Finally, there are pharmacological conditions under which choline levels and ACh release are dissociated such as following administration of Ch transport blockers (Ch levels are increased, ACh release is diminished) or acetylcholinesterase inhibitors (Ch levels can be reduced whereas ACh efflux is enhanced). Thus, a microelectrode sensitive to ACh itself, and not just choline, would provide a more direct method for studying the rapid dynamics of ACh release.

We have recently reported the development of a multichannel microelectrode array (MEA) that is sensitive to both ACh and to Ch (Bruno *et al*., 2006b). In this article we present a more thorough functional validation of the MEA *in vivo*. Self-referencing techniques allow one to isolate the current generated by the release of ACh. We conducted three experiments, in anaesthetized rats, in order to document the MEA's ability to rapidly measure changes in ACh release. First, we determined the ability of the MEA to detect exogenously administered ACh that is pressure ejected into prefrontal cortex (PFC). Second, we determined the ability of the MEA to measure the release of endogenous cortical ACh following local depolarization with a high concentration of K^+. Finally, we demonstrated the MEA's capacity to detect the release of ACh following pressure ejections of nicotine into PFC.

Materials and methods

Subjects

Male Fisher/Brown Norway F1 hybrid (Harlan Sprague–Dawley, Indianapolis, IN, USA) and Wistar (Charles River, Wilmington, MA, USA) rats weighing between 250 and 400 g were used as subjects in these experiments. Animals were maintained in a temperature and humidity controlled room on a 12-h light : 12-h dark cycle (lights on at 06:00 h) and individually housed in plastic cages lined with corn cob bedding (Harlan Teklad, Madison, WI, USA). Animals had access to food and water *ad libitum*. All procedures involving animals were approved by The Ohio State University Institutional Animal Care and Use Committee in accordance with the NIH Guide for the Care and Use of Laboratory Animals.

Coating of ACh-Ch-sensitive microelectrode

The MEA has four 15 × 333 μm platinum (Pt) recording sites arranged in pairs beginning approximately 100 μm from the electrode tip (see Fig. 1). The two microelectrode sites sensitive to only choline (Ch) were coated with a solution (100 nL) containing choline oxidase (ChOX, 0.13 Units/μL), bovine serum albumin (3%, BSA), and glutaraldehyde (0.375%). The solution was made in HPLC-grade water and applied using a 1.0-μL syringe (Hamilton Co., Reno, NV, USA). The two sites sensitive to both ACh and Ch were also coated with the solution mentioned above to which acetylcholinesterase (AChE, 0.13 Units/μL) was also added. After coating, microelectrodes were dried at room temperature for at least 48 h. After drying, microelectrodes were stored in a dessicator until use.

Plating of ACh-Ch-sensitive microelectrode

On the day of testing, enzyme-coated microelectrodes were electropolymerized (+0.5 V vs. Ag/Ag^+ reference) in a phosphate-buffered

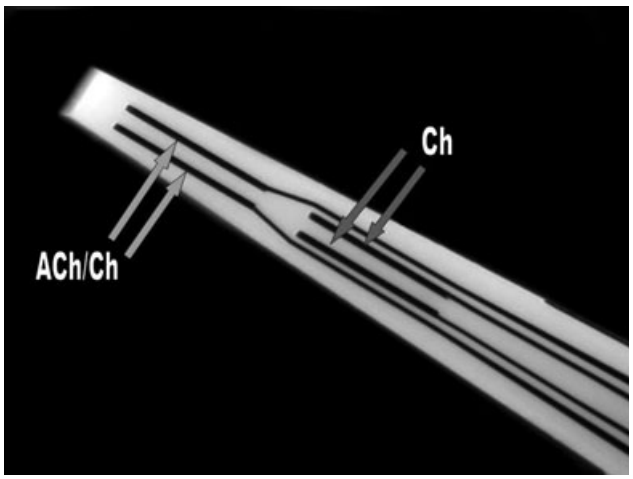

FIG. 1. High magnification photomicrograph of the recording sites of the ACh-sensitive microelectrode array (MEA) illustrating the two pairs of Pt channels. The first pair, located 100 μm from the tip of the MEA was sensitive to both ACh- and Ch-based signals whereas the second pair, located 100 μm up the shaft of the MEA was sensitive to only Ch-based signals (see Materials and methods for coating details). Each recording channel is 15 × 333 μm in area and is located 30 μm away from the other member of the pair.

saline (PBS, 0.05 M) bath (50 mL) containing *m*-polyphenylene diamine (*m*-PD, 5.0 mM) for one hour to create an exclusion layer designed to prevent, on the basis of size, potential interferents such as ascorbic acid and catecholamines from contacting the recording sites of the microelectrode (Lowry *et al*., 1998; Mitchell, 2004). Oxygen was removed from the PBS bath by bubbling the solution with nitrogen gas for 25 min prior to the addition of *m*-PD to the bath.

Detection of ACh- and Ch-generated signals

Figure 1 is a high magnification photograph of the tip of the MEA. The photograph shows the four 15 × 333 μm Pt recording sites beginning approximately 100 μm from the tip of the microelectrode. The two sites closer to the tip are sensitive to both ACh and Ch whereas the remaining two sites are sensitive only to Ch.

The detection scheme that generates the ACh- and Ch-linked current changes is depicted in Fig. 2. The various coatings of the Pt electrode surface are indicated by the shaded columns. The recording sites are coated with choline oxidase (ChOX, the distal two sites) or ChOX + acetylcholinesterase (AChE, the two sites closest to the tip). Following the enzyme coating, an exclusion layer of *m*-PD is electropolymerized on the microelectrode surface. ACh is hydrolysed at the surface of the microelectrode (and locally via endogenous AChE surrounding the electrode tip) generating Ch and acetate. The Ch is oxidized on the microelectrode surface and results in the production of the reporting molecule H_2O_2. H_2O_2 passes through the *m*-PD barrier and is then oxidized on the Pt surface and the resulting current change is detected, amplified and processed by the FAST-16 software (Quanteon, LLC, Lexington, KY, USA). Figure 2 also schematizes the targeted positioning of the MEA within the prefrontal cortex. A more complete discussion of the equipment and interconnections utilized in capturing signals from the MEA can be found in our previous publications (Burmeister & Gerhardt, 2006; Hascup *et al*., 2006).

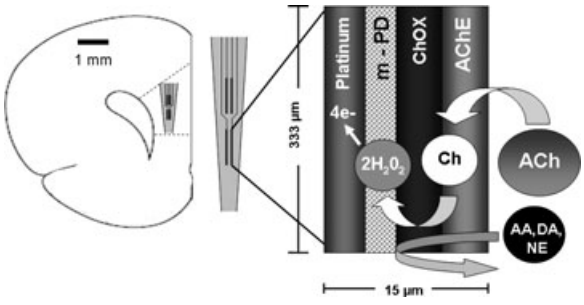

FIG. 2. Illustration depicting the enzyme coatings and transduction scheme involved in the oxidation of H_2O_2, the reporting molecule detected at the Pt surface of the MEA. Recording sites were coated with either ChOX (Ch-sensitive sites) or ChOX + AChE (ACh/Ch-sensitive sites). This particular illustration depicts the coatings present on the ACh/Ch-sensitive site of the MEA. The two enzymes are covalently bound to the surface of the electrode with a BSA-glutaraldehyde solution. ACh is hydrolysed to choline. The subsequent oxidation of choline generates two molecules of H_2O_2 for every molecule of choline. Following the enzyme coatings, *m*-PD is electropolymerized onto the surface of the Pt recording channel. *m*-PD plating provides a barrier that effectively blocks access of potential electroactive interferents (such as AA, DA, and NE) to the surface of the electrode. H_2O_2 freely passes through the *m*-PD barrier and is oxidized at the Pt surface at a constant potential of +0.7 V. The figure also depicts a schematic coronal section illustrating the positioning of the tip of the MEA in the prefrontal cortex.

In vitro *calibration of microelectrodes*

Microelectrodes were calibrated using the FAST-16 electrochemical recording system prior to implantation. Amperometry was conducted using an applied potential of +0.7 V vs. a Ag/Ag^+ reference electrode. Calibrations were performed in a stirred solution of 0.05 M PBS (40 mL) at 37 °C. After stabilization, aliquots of stock solutions of ascorbic acid (20 mM), ACh (20 mM), Ch (20 mM), DA (20 mM) and NE (2 mM) were added to the calibration beaker so the final concentrations of each solution tested were: 250 μM ascorbic acid, 20, 40, and 60 μM ACh, 20 μM Ch, and 20 μM DA and 2 μM NE. Amperometric signals were acquired at a rate of 1.0 Hz (> 80 000 points/channel/s). The slope, limit of detection (LOD), and linearity (R^2) for ACh and Ch, as well as the selectivity ratio for ascorbic acid, DA, and NE were calculated. The Ch slopes between pairs of sites were also determined, and microelectrode arrays (MEAs) were excluded from use if the Ch slopes between channels 1 and 3 or between 2 and 4 deviated from one another by more than 20%. In order to be used for subsequent *in vivo* recordings, the MEAs had to conform to the following calibration criteria (single electrode mode): (i) similar background currents (i.e. no greater than 10 pA) on all channels prior to the addition of any analyte during calibration, (ii) linear response to increasing concentrations of ACh ($R^2 = 0.998$), and (iii) highly selective to ACh as compared to either AA or DA (100 : 1).

In vivo *recordings*

Animals ($n = 5$) were anaesthetized using urethane (1.25 g/kg i.p.) and implanted with the ACh microelectrode into the mPFC (in mm from bregma: AP +2.7, ML ± 0.7, DV −4.2, hemispheres counterbalanced). Coordinates were determined from the atlas of Paxinos & Watson (1998). Animals' body temperatures were maintained at 37 °C throughout the experiment using a heating pad. The Ag/AgCl reference electrode was implanted in a contralateral site distant from the recording site.

Single barrel glass capillary micropipettes were pulled using a micropipette puller (David Kopf Instruments, Tujunga, CA, USA) and bumped to an inner diameter of 10–20 μm. Micropipettes were first filled with an ejection solution (saline, ACh, KCl, or nicotine) and then fixed to the microelectrode using sticky wax (Kerr, Romulus, MI, USA) so that pipettes were located 50–100 μm away from the surface of the MEA and equidistant from the two pairs of recording sites.

The microelectrode/micropipette assembly was slowly lowered into the mPFC and allowed to reach a stable baseline (~2-h postinsertion) before initiating pressure ejections. Sets of four ejections of KCl (70 mM) were made at 2-min intervals. The initial four ejections were of 40 nL followed, 30 min later, by four ejections of 160 nL. The concentration and volumes of KCl were taken from our previous studies on evoked glutamate release in striatum and cortex (Burmeister *et al*., 2002; Day *et al*., 2006). The solution in the micropipette was changed to ACh (10 mM) and, 60 min later, an additional set of four pressure ejections (40 nL) were delivered. Pressure ejections of KCl were always conducted prior to ACh as pilot studies indicated that the response to KCl was a fraction of that of the response to exogenously applied ACh. We delivered the less potent stimulus (KCl) first in lieu of concerns about autoreceptor-induced decreases in the excitability of the cortical cholinergic terminals (Ibouz *et al*., 1999) following the delivery of higher concentrations of exogenous ACh. Again, amperometric data were acquired at a frequency of 1.0 Hz. In several animals, the vehicle solution of iso-osmotic saline was pressure

ejected prior to the KCl ejections in order to confirm that the current changes seen at the ACh/Ch- and Ch-sensitive sites was not due to the ejection of fluid *per se*.

An additional group of rats ($n = 5$) were used to measure the ability of nicotine to stimulate ACh release. For this experiment a microdialysis probe was positioned 200–300 μm away from the recording sites of the MEA. Microdialysis probes were implanted 3 h before beginning baseline collections; microelectrode/micropipette assemblies were implanted no more than 1 h after dialysis probe implantation. Microdialysis probes were continually perfused with artificial cerebral spinal fluid (aCSF, containing in mM: NaCl 166.5, $NaHCO_3$ 27.5, KCL 2.4, $CaCl_2$ 1.2, Na_2SO_4 0.5, KH_2PO_4 0.5, $MgCl_2$, and glucose 0.8; pH 7.1) at a rate of 1.25 μL/min throughout the duration of the experiment. For nicotine/neostigmine experiments, four baseline microdialysis collections (15 min each) were taken before a series of four pressure ejections of nicotine (1.0 mM, 80 nL). Following baseline collections and the initial four nicotine ejections, dialysis lines were switched from a syringe containing aCSF to one containing aCSF + neostigmine (10.0 μM). Neostigmine was perfused through the dialysis probe for a total of 90 min before an additional series of four ejections of nicotine was delivered.

Histology

At the conclusion of each experiment, animals were transcardially perfused with heparinized saline (0.9%) followed by formalin (10%). Brains were removed and stored in formalin for 24 h, and then transferred to a sucrose solution (30%) for at least three days. Brains were sectioned using a cryostat; sagittal sections (50 μm) were mounted on slides, stained using Cresyl Violet, and examined under a light microscope for verification of microelectrode or microelectrode/dialysis probe placements.

Self-referencing of the microelectrode signals

Changes in current that directly reflect the oxidation of H_2O_2 generated by the hydrolysis of ACh can be isolated using a self-referencing procedure against the adjacent site (channel) that is only sensitive to current generated by the oxidation of Ch. This procedure normalizes the recording sites to account for potential coating and electrode response differences to Ch or H_2O_2. The normalized Ch channel response is then subtracted from the normalized ACh channel response. This removes the contribution of current generated by Ch alone from the ACh signal, leaving a current that is due exclusively to ACh. The subtraction product is then divided by the self-referencing slope (nA/μM) and this converts the electrode response to μM equivalents.

Data analysis

Measures subjected to subsequent data analyses included peak amplitude (μM equivalent of ACh), clearance rate of ACh (μM/s), T_{80}, the time(s) required for the ACh signal to decline by 80% of the maximum amplitude, and ACh efflux in dialysate (fmol/μL). The *in situ* electrochemical values were calculated from the self-referenced data, allowing the isolation of the ACh signal. An initial repeated measure one-way ANOVA was conducted for each volume of KCl, ACh, and nicotine in order to determine if the effects were stable and reproducible across ejections. In the absence of any significant differences among the four pressure ejections of a given volume, an overall significant ANOVA, followed by various pairwise comparisons designed to test for the effects of different volume-dependent effects (KCl experiment), was conducted using the third ejection of each volume (40, 160 nL).

Due to uncertainties surrounding the distribution of pre-neostigmine and nicotine-induced signals, nonparametric statistics [Wilcoxin test for dependent samples (Bruning & Kintz, 1997)] were utilized to evaluate the effects of neostigmine perfusion on the amplitude, clearance rate and T_{80} of the ACh signal. ACh efflux (fmol/μL) from the microdialysis study was analysed using a repeated measures ANOVA in order to determine the effects of neostigmine on extracellular levels of ACh. Statistical significance for all analyses was defined as $P = 0.05$.

Results

In vitro calibration

Representative *in vitro* calibration recordings are depicted in Fig. 3. This figure illustrates three different tracings following the administration of ACh, Ch and several potential interferents. The top tracing is from a site sensitive to current generated by both ACh and Ch. The middle tracing is from the adjacent site that is sensitive only to Ch. The progressive additions to the ACh concentration in the beaker (by 20 μM increments) resulted in a linear step-wise increase in current on the ACh/Ch-sensitive site. Additions of ACh did not result in significant current changes on the Ch-sensitive site. As expected, the administration of Ch (20 μM) produced similar changes in current on both the ACh/Ch- and Ch-sensitive sites. The bottom tracing contains the self-referenced subtraction data and isolates current change due exclusively to the hydrolysis of ACh. Administration of ACh resulted in a linear increase in signal with negligible effects of Ch or the potential interferents (typical selectivity of 100 : 1). The administra-

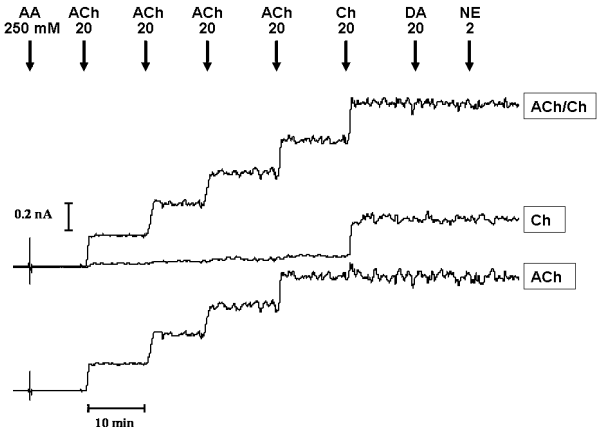

FIG. 3. Representative current tracings from an *in vitro* calibration of the MEA prior to insertion into PFC. The escalating tracing on the top depicts the current recorded from the site that is sensitive to both ACh and Ch. The middle tracing is from the site that is sensitive to only Ch. The bottom tracing, subtracted, represents the self-referenced difference between the top two tracings and highlights current generated exclusively by ACh (see Materials and methods for details). At the top of the figure are the substances and the concentrations (mM) in the calibration beaker. Both sites were relatively insensitive to a high concentration of AA (250 μM), documenting the effectiveness of the *m*-PD plating. Progressive additions of ACh (in 20-μM increments) produced a linear increase in the signal in the top tracing with very little effect on the Ch-sensitive site. As expected, the addition of Ch (20 μM) resulted in a similar signal at both the ACh/Ch and Ch sites. Administration of DA (20 μM) or NE (2 μM) produced only marginal changes in current, again illustrating the effectiveness of *m*-PD plating.

tion of ascorbic acid (AA, 250 μM), dopamine (DA, 20 μM) or norepinephrine (NE, 2.0 μM), all potential *in vivo* interferents in prefrontal cortex, resulted in negligible increases in current on any of the three tracings. This demonstrates that *m*-PD effectively blocks these compounds from reaching the surface of the MEA. An analysis of the *in vitro* calibration data from all MEAs used in these experiments revealed a mean (± SEM) sensitivity of −9.3 ± 1.4 pA/μM ACh and L.O.D. of 0.65 ± 0.22 μM ACh in the single electrode mode and −39.3 ± 3.9 pA/μM and 0.08 ± 0.02 μM in the self-referenced mode.

Placements of microelectrode/micropipette assemblies

Figure 4 is a photomicrograph of a representative placement of the microelectrode/micropipette assembly. The saggital section depicts a representative placement from the combined microdialysis and micropipette/microelectrode assemblies used for the perfusion of neostigmine coupled with pressure ejections of nicotine or saline. The placements of the microelectrode alone, in the experiments involving ACh or KCl ejections, were similar to those placements depicted by the microelectrode in this figure. The head of the microdialysis probe was orientated rostrally at a 30° angle and the membrane terminated within 200–300 μm of the MEA's recording sites. The differences in the extent of tissue disruption produced by insertion of the microdialysis probe vs. the MEA are quite pronounced. The minimal degree of tissue damage produced by the MEA has been noted previously (Talauliker *et al*., 2005).

In vivo *detection of pressure ejected ACh*

Pressure ejections of ACh led to discrete, rapid changes in current measured at the surface of the MEA. Representative signals, expressed as μM equivalents, generated by four consecutive pressure ejections are illustrated in Fig. 5. As in Fig. 3, the top tracing is one recorded from the site sensitive to both ACh and Ch. The middle tracing is from the site sensitive only to Ch. The bottom tracing represents the self-referenced subtraction and isolates the signal generated exclusively from the hydrolysis of ACh. In each case, pressure ejections produced clear ACh signals that reached peak amplitude (mean, 51.2 ± 16.5 μM) in 1–2 s and were cleared (mean, 19.3 ± 8.2 μM/s) rapidly (mean T_{80}, 10.6 ± 2.2 s). A comparison among the four ejections revealed that peak amplitude, clearance rate, and T_{80} were very reproducible (all *P*s > 0.05).

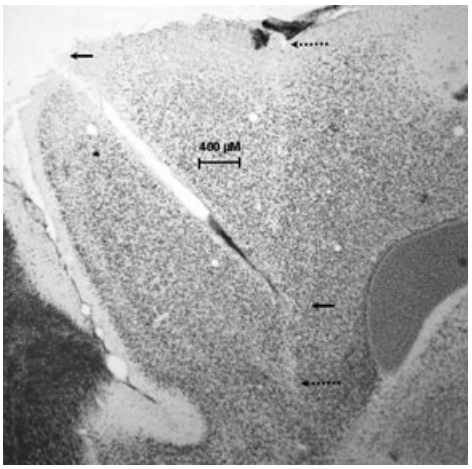

FIG. 4. Representative photomicrograph depicting the placements of the MEA (length marked by the broken arrows) and the microdialysis probe (length marked by the solid arrows) in PFC. The placements of the MEA in the initial experiments on ACh and KCl ejections were very similar to that presented here. The sagittal section illustrates that the tip of the microdialysis probe, orientated at a 30° angle, terminated in close proximity to the recording sites of the MEA. The modest tissue disruption introduced by the MEA, relative to that produced by the microdialysis probe, is readily apparent.

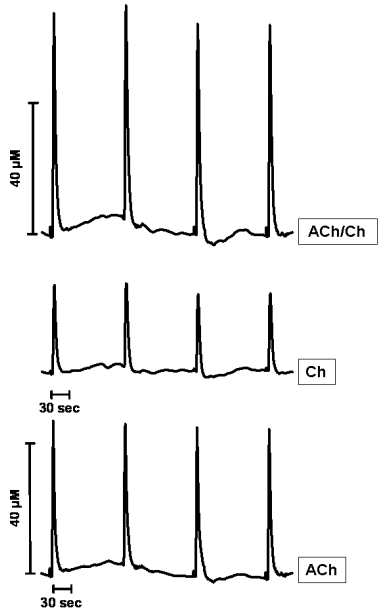

FIG. 5. Representative current tracings following four pressure ejections (40 nL) of ACh (10 mM) into the PFC of an anaesthetized rat. As in Fig. 3, the top tracing is from the site sensitive to both ACh and Ch, the middle tracing is from the site sensitive to only Ch and the bottom trace the self-referenced output highlighting current changes due exclusively to the hydrolysis of ACh. In all tracings, the rise in current began very soon after the pressure ejection, reaching peak amplitude within 1–2 s. The scale bar indicates a conversion of current change to 40 μM equivalents of ACh or Ch. The ACh and Ch signals were rapidly cleared by 80% of peak amplitude within 4–11 s.

In vivo detection of endogenously released ACh

The ACh-sensitive MEA was also capable of detecting signals generated from the release of endogenous ACh. Representative signals, expressed as μM equivalents, generated by pressure ejections of two volumes of KCl (70 mM) are illustrated in Fig. 6. The bottom tracing represents the self-referenced subtraction and isolates the signal generated exclusively from the hydrolysis of ACh. As was the case with ejections of ACh, local depolarizations following pressure ejections of KCl produced clear signals that reached peak amplitude in 1–2 s and were cleared rapidly (T_{80}, 4–10 s). Again, there were no significant differences among the four ejections in any of the dependent measures (all *P*s > 0.05).

An analysis of the signals from the third pressure ejection of each volume revealed that the peak amplitude of the signals (40 nL, 4.34 ± 0.91 μM; 160 nL, 7.99 ± 1.22 μM) were volume-dependent ($F_{1,4} = 11.13$, $P = 0.029$). The analysis also revealed a trend ($F_{1,4} = 4.29$, $P = 0.10$) towards volume-dependent differences in clearance rate (40 nL, 0.3 ± 0.2 μM/ s; 160 nL, 0.7 ± 0.3 μM/s). The two volumes required similar times to reach the T_{80} point (40 nL, 7.4 ± 2.5 s; 160 nL, 6.4 ± 2.5 s).

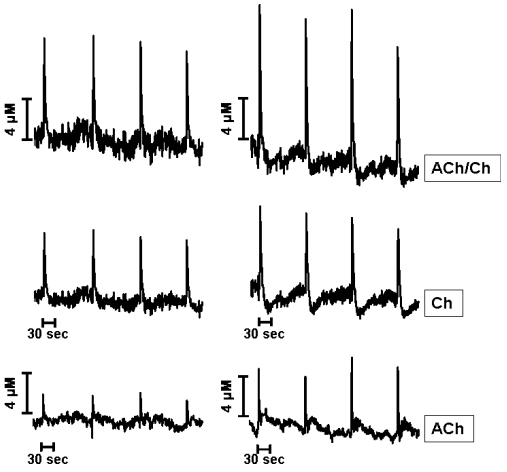

FIG. 6. Representative current tracings following pressure ejections (40 nL, left or 160 nL, right) of KCl (70 mM) into the PFC of an anaesthetized rat. As in previous figures, the top tracing is from the site sensitive to both ACh and Ch, the middle tracing is from the site sensitive to only Ch and the bottom trace the self-referenced output highlighting current changes due exclusively to the hydrolysis of ACh. The amplitude of the self-referenced ACh signals was clearly dependent upon the volume of KCl ejected. In all tracings, the increase in current began very soon after the pressure ejection, reaching peak amplitude within 1–2 s. The scale bar indicates a conversion of current change to μM equivalents of ACh or Ch. The ACh and Ch signals were rapidly cleared by 80% within 4–11 s.

Nicotine-induced release of cortical ACh

The final experiment was designed to further validate the ACh-sensitive MEA by assessing its ability to detect ACh release following local ejections of nicotine. Figure 7 (top panel) illustrates a representative recording of the effects of local pressure ejections of nicotine (1.0 mM) on the self-referenced ACh signal in PFC. The results from the first four ejections of nicotine (i.e. pre-neostigmine) appear as the first four peaks on the tracings. Nicotine-induced ACh signals, like those seen following ACh or KCl, rise rapidly to peak amplitude and then are rapidly cleared to baseline. An inspection of Fig. 7 (top panel) and an analysis of the group data reveal that the peak amplitude, clearance rates and T_{80} values were similar among the four ejections (all *P*s > 0.05). Thus, the statistical analyses on the group data were conducted using the results of the third pressure ejection. Pressure ejections of nicotine resulted in marked increases in the amplitude of the ACh signal (4.40 ± 1.58 μM). These signals were cleared at a rate 2.18 ± 1.36 μM/s, reaching 20% of maximum (i.e. T_{80}) by 6.0 ± 1.5 s (see inset).

The representative data depicted in Fig. 7 (top panel, right) also illustrate the effects of intracortical perfusion of the AChE inhibitor neostigmine (10 μM) on the nicotine-induced ACh signal. The analysis revealed a marked attenuation of nicotine's peak amplitude to 1.27 ± 0.32 μM ($Z = -2.023$, one-tailed test, $P = 0.02$; 39–99% attenuation; mean = 66 ± 12%) following neostigmine. Mean (± SEM) data for clearance rate ($P < 0.05$) and T_{80} ($P > 0.05$) are depicted in the inset. As expected following such a marked reduction in ACh signal, statistical analyses revealed the clearance rate was reduced following perfusion with neostigmine ($Z = -2.023$, $P = 0.04$) whereas there was a trend for T_{80} to increase ($P = 0.07$).

As expected, HPLC analyses of ACh efflux in the vicinity of the dialysis probe/MEA assembly, an indication of neostigmine's ability to inhibit AChE, revealed highly significant increases in ACh efflux (mean 9686 ± 4331%), relative to pre-neostigmine levels, for each of the five rats.

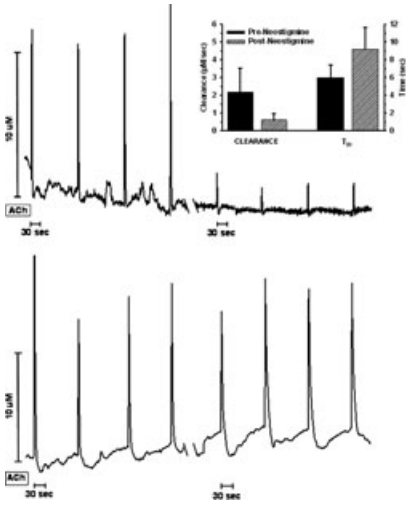

FIG. 7. Representative self-referenced current tracings of nicotine-induced ACh release prior to the local administration of the AChE inhibitor neostigmine (first 4 peaks on the top tracing) and after (final four peaks on the top tracing) in the PFC of an anaesthetized rat. In the top tracing, pressure ejections of nicotine (1 mM) evoked large and consistent increases in the ACh signal that were markedly attenuated 90 min after neostigmine, demonstrating that the signal derived from ACh is dependent upon the hydrolysis of ACh via AChE. Neostigmine (10 μM) was perfused via reverse dialysis (probe positioned 500 μM away from the surface of the MEA, see Fig. 4). The bottom tracing is a time control showing that in the absence of neostigmine, nicotine-induced signal remained consistent throughout the entire duration of the experiment ruling out nicotine receptor desensitization or a decrease in electrode performance. The break in the X-axis excludes the initial 90 minutes where neostigmine was perfused prior to nicotine administration. The scale bar indicates a conversion of current change to μM equivalents of ACh. The inset in the top right corner of the figure displays the clearance rate and T_{80} values pre- and post-neostigmine.

The marked attenuation of nicotine following neostigmine perfusion (Fig. 7, top panel) did not reflect a time-dependent desensitization of the nicotine receptor or declines in the sensitivity of the MEA. Figure 7 (bottom panel) illustrates the effects of a representative timed-control in which the temporal aspects of the experiment were maintained but aCSF was perfused rather than neostigmine. The amplitude and clearance parameters of the self-referenced ACh signal detected in the second cluster of four nicotine ejections was no different than those seen in the initial series of drug ejections.

Discussion

These experiments were designed to validate the ACh-sensitive microelectrode array (MEA) as a method for the rapid, *in situ* measurement of cortical ACh release. Four observations are reported in this manuscript. First, the MEA is sensitive to ACh in the low micromolar range and the detection is selective against several known electroactive interferents (ascorbate, DA and NE) that could be encountered in brain tissue. Second, when implanted into the mPFC, the ACh-sensitive MEA is able to rapidly detect exogenously administered ACh with second-to-second resolution. Third, the ACh-sensitive MEA detects volume-dependent changes in endogenously released ACh following local depolarization with KCl or stimulation with nicotine. Finally, nicotine-induced ACh signals reflect the hydrolysis of newly released ACh as the amplitude of the signal is markedly attenuated by inhibition of AChE in the area surrounding the MEA. The discussion that follows addresses several more specific issues raised by these observations.

The nature of the signals recorded at the background Ch-sensitive site

Pressure ejections of ACh, KCl or nicotine resulted in clearly discernible signals with a rapid rise (~1 s) to peak amplitude and then a more protracted clearance (4–12 s) to baseline on both the Ch- and ACh/Ch-sensitive sites. The interpretation that this signal, at the Ch-sensitive site, represents the detection of a current generated by the sequential oxidation of choline and H_2O_2 is consistent with previous results using an identical MEA that consists of a Ch-sensitive site and a sentinel site that is only coated with BSA and glutaraldehyde (Parikh *et al*., 2004; Parikh & Sarter, 2006). In these studies, pressure ejection of KCl or the muscarinic antagonist scopolamine produced signals similar to those we report from our Ch-sensitive site. Moreover, these stimulated signals were attenuated by blockade of voltage-dependent impulse flow by TTX and were not evident on the sentinel site. While the previous TTX data, as well as the neostigmine data reported in this manuscript, suggest that this stimulated Ch signal is the result of the release of ACh from nerve terminals and its subsequent hydrolysis to Ch by AChE, the detection of Ch represents an indirect measure of ACh release. In contrast to ACh, extracellular levels of Ch in brain can be markedly influenced by non-neuronal factors (Zeisel, 1981). The current MEA design with closely apposed ACh/Ch- and Ch-sensitive sites offers, for the first time, the opportunity to directly measure ACh release *in situ*, with second-by-second resolution.

The nature of the ACh-derived signal

The coating scheme of the MEA and the self-referencing procedure used in this experiment allows for the isolation of current generated from newly released ACh from current generated from choline and other electroactive species. We refer to the product of this self-referencing as the ACh signal. Several observations collectively suggest that this signal is due exclusively to the release of ACh from nerve terminals in close proximity to the MEA. First, the amplitude of the signals on the ACh/Ch-sensitive sites is invariably larger than the signals on the Ch-sensitive sites, suggesting an additional source of oxidizeable choline – namely the hydrolysis of ACh at the MEA surface. Second, large-scale inhibition of the hydrolysis of ACh leads to a near-total attenuation of the nicotine-induced ACh signal. Third, recent unpublished observations demonstrate that inhibition of Na^+-gated impulse flow with local perfusions of TTX eliminate nicotine-induced ACh signals yet have little effect on signals generated by control ejections of choline.

Of course, the validity of the self-referencing procedure hinges upon the extent to which the two recording sites (ACh/Ch vs. Ch) are comparable with respect to (i) the sensitivity to choline and ultimately H_2O_2, as well as (ii) the dynamics of cholinergic transmission in the specific brain regions in which the two sites are located (100 μm from one another). With respect to sensitivity, we select recording channels on the basis of similar Ch slopes obtained during the *in vitro* calibration. We then adjust for any small differences in slopes by normalizing the sensitivity to Ch at the ACh/Ch site with the sensitivity to Ch at the Ch site (i.e. self-referencing). The issue of regional differences in cholinergic transmission between the precise locations of the ACh/Ch and Ch site is a more difficult issue to control. Naturally, the closer the two sites are to one another, the more valid the self-referencing procedure. To that end, we are currently testing an instrumented enzyme coating procedure that will allow for the differential coating of side-by-side members of a pair (30 μm apart but located at the same dorsal-ventral position in brain) as opposed to a member from each of the two pairs of sites (100 μm apart). We have also recently designed an MEA geometry that has recording channels on both sides of the ceramic platform (~125 μm in thickness). These procedures should minimize the likelihood that the two recording sites are sampling from functionally different subregions thereby enhancing the validity of the self-referencing procedure.

In one of the experiments described above, we report that the ACh signal varied as a function of the volume of KCl that was pressure ejected onto the MEA. In these initial validation experiments we chose to utilize a single micropipette so that we could best control for the critical position of the tip of the micropipette relative to the pairs of recording channels on the MEA. We also wanted to minimize the chances of disturbing this spatial relationship by changing the solutions contained within the micropipette. Thus, we varied the magnitude of the KCl stimulus by changing volume rather than concentration that was pressure ejected. We obtained volume-dependent effects on amplitude (μM equivalents) with a trend toward enhanced clearance rates. These *in vivo* effects were linear but the slope of the volume–amplitude curves was low (i.e. 0.02–0.4). This slope might have been reduced by the differential effects of the two volumes on diffusion of KCl away from the surface of the recording site. Recently, using double-barrel micropipette/MEA assemblies (in which concentration and volume are unconfounded) we have demonstrated clear concentration-dependent effect of nicotine-induced ACh signals with slopes that are significantly higher (~0.7, unpublished observations).

Ongoing experiments using the ACh-sensitive MEA

The present experiments were designed to validate the ACh-sensitive MEA as means for measuring *in vivo* ACh release with a temporal and spatial resolution not provided by conventional methodologies. The anaesthetized rat provided an ideal model for optimizing the various coating and recording parameters needed to reliably measure ACh release in prefrontal cortex. Our ongoing research focuses on the use of the ACh-sensitive MEA in measuring cortical ACh release in awake, freely moving rats exposed to novel sensory stimuli or those stimuli with incentive value as a result of being associated with reward. We have recently reported that a brief exposure to a startle-producing auditory stimulus (three 100 dB tones, delivered over 3 s) or a biologically salient odour (the soiled bedding of a female rat for 5 min) results in a rapid increase in prefrontal ACh release (Bruno *et al*., 2006a). The increase in ACh signal in response to the auditory startle stimulus was evident within 1 s after the presentation of the tone and returned to baseline as soon as 3 s later. Moreover, repeated exposures to the tone produced progressively smaller increases in cortical ACh release until, by the eighth presentation no increase in release was elicited. Exposure to the salient odour produced an increase in the prefrontal ACh signal. The signal emerged above baseline at approximately 2 min after exposure, reached maximum amplitude (~0.4 μM) at 5–6 min and gradually declined to baseline over the ensuing 20 min.

While each of these sensory events might ultimately produce a measurable change in ACh efflux during a 10–15 min dialysis collection (see Acquas *et al*., 1996), the detection of such rapid changes in cortical ACh release as well as the progressive nature of the rise and fall in ACh release would clearly not be possible using the temporally more sluggish method of microdialysis. Obviously, the ultimate heuristic leverage afforded by the ACh-sensitive microelectrode will be realized when applied in animals engaged in behavioural paradigms with discrete behavioural responses following rapidly changing task contingencies. To date, this type of analysis has been

applied to studies on the relationship between forebrain DA systems and stressors (Richardson & Gratton, 1998) or reward (Phillips *et al.*, 2003; Carelli & Wightman, 2004). Given the documented relationship between cortical cholinergic transmission and attention (Sarter *et al.*, 2003, 2005), the use of the ACh-sensitive microelectrode to study the dynamics of ACh release associated with different response types and stages of attentional processing may provide insights that are not possible with conventional methodologies.

Acknowledgements

Contract grant sponsor: NIDA #DA019502. We wish to thank Catherine Werner for her technical assistance with the conduct of many of these experiments.

Abbreviations

AA, ascorbic acid; ACh, acetylcholine; AChE, acetylcholinesterase; aCSF, artificial cerebral spinal fluid; Ch, choline; ChOX, choline oxidase; DA, dopamine; H_2O_2, hydrogen peroxide; NE, norepinephrine; *m*-PD, *m*-polyphenylene diamine; MEA, microelectrode array; PBS, phosphate-buffered saline; PFC, prefrontal cortex; Pt, platinum.

References

Acquas, E., Wilson, C. & Fibiger, H.C. (1996) Conditioned and unconditioned stimuli increase frontral cortical and hippocampal acetylcholine release: effects of novelty, habituation, and fear. *J. Neurosci.*, **16**, 3089–3096.

Araki, W. & Wurtman, R.J. (1998) How is membrane phospholipids biosythesis controlled in neural tissue? *J. Neurochem. Res.*, **51**, 667–674.

Arnold, H.M., Burk, J.A., Hodgson, E.M., Sarter, M. & Bruno, J.P. (2002) Differential cortical acetylcholine release in rats performing a sustained attention task versus behavioral control tasks that do not explicitly tax attention. *Neuroscience*, **114**, 451–460.

Bruning, J.L. & Kintz, B.L. (1977) *Computational Handbook of Statistics*, 2nd Edn. Soctt, Foresman and Co, Glenview, IL.

Bruno, J.P., Gash, C., Martin, B., Gerhardt, G.A., Pomerleau, F., Huettl, P. & Burmeister, J. (2006a) Sensory- and drug-induced cortical ACh release on a second-by-second basis in awake rats. *Soc. Neurosci. Abstr.*, 486.1.

Bruno, J.P., Sarter, M., Gash, C. & Parikh, V. (2006b) Choline- and acetylcholine-sensitive microelectrodes. In Grimes, C.A., Dickey, E.C & Pishko V., (Eds), *Encyclopedia of Sensors*. American Scientific Publishers, Stevenson Ranch, CA, USA.

Bruno, J.P., Sarter, M., Moore Arnold, H. & Himmelheber, A.M. (1999) *In vivo* neurochemical correlates of cognitive processes: methodological and conceptual challenges. *Rev. Neurosci.*, **10**, 25–48.

Burmeister, J.J. & Gerhardt, G.A. (2006) Neurochemical arrays. In: Grimes, C., Dickey, E. & Pishko M.V., (Eds), *Neurochemical arrays in Encyclopedia of Sensors*, **Vol. 6**. American Scientific Publishers, Stevenson Rancy, CA.

Burmeister, J.J., Palmer, M. & Gerhardt, G.A. (2003) Ceramic-based multisite microelectrode array for rapid choline measures in brain tissue. *Anal. Chim. Acta*, **481**, 65–74.

Burmeister, J.J., Pomerleau, F., Palmer, M., Day, B.K., Huettl, P. & Gerhardt, G.A. (2002) Improved ceramic-based multisite microelectrode for rapid measurements of l glutamate in the CNS. *J. Neurosci. Meth.*, **119**, 163–171.

Carelli, R.M. & Wightman, R.M. (2004) Functional microcircuitry in the accumbens underlying drug addiction: insights from real-time signaling during behavior. *Curr. Opin. Neurobiol.*, **14**, 763–768.

Cui, J., Kulagina, N.V. & Michael, A.C. (2001) Pharmacological evidence for the selectivity of *in vivo* signals obtained with enzyme-based electrochemical sensors. *J. Neurosci. Meth.*, **104**, 183–189.

Dalley, J.W., Cardinal, R.N. & Robbins, T.W. (2004) Prefrontal executive and cognitive functions in rodents: neural and neurochemical substrates. *Neurosci. Biobehav. Rev.*, **28**, 771–784.

Dalley, J.W., McGaughy, J., O'Connell, M.T., Cardinal, R.N., Levita, L. & Robbins, T.W. (2001) Distinct changes in cortical acetylcholine and noradrenaline efflux during contingent and noncontingent performance of a visual attention task. *J. Neurochem.*, **21**, 4908–4914.

Day, J.C., Kornecook, T.J. & Quirion, R. (2001) Application of *in vivo* microdialysis to the study of cholinergic systems. *Methods*, **23**, 21–39.

Day, B.K., Pomerleau, F., Burmeister, J.J., Huettl, P. & Gerhardt, G.A. (2006) Microelectrode array studies of basal and postassium-evoked release of 1-glutamate in the anaesthetized rat brain. *J. Neurochem.*, **96**, 1626–1635.

Everitt, B.J. & Robbins, T.W. (1997) Central cholinergic systems and cognition. *Ann. Rev. Psychol.*, **48**, 649–684.

Garguilo, M.G. & Michael, A.C. (1996) Amperometric microsensors for monitoring choline in the extracellular fluid of brain. *J. Neurosci. Meth.*, **70**, 73–82.

Gobert, A., Di Cara, B., Cistarelli, L. & Millan, M.J. (2003) Piribedil enhances frontocortical and hippocampal release of acetylcholine in freely moving rats by blockade of alpha 2A-adrenoreceptors: a dialysis comparison to talipexole and quinelorane in the absence of acetylcholinesterase inhibitors. *J. Pharmacol. Exp. Ther.*, **305**, 338–346.

Golmayo, L., Nunez, A. & Zaborszky, L. (2003) Electrophysiological evidence for the existence of a posterior cortical-prefrontal-basal forebrain circuitry in modulating sensory responses in visual and somatosensory rat cortical areas. *Neuroscience*, **119**, 597–609.

Hascup, K.N., Rutherford, E.C., Quintero, J.E., Day, B.K., Nickell, J.R., Pomerleau, F., Huettl, P., Burmeister, J.J. & Gerhardt, G.A. (2006) Second-by-second measures of L-glutamate and other neurotransmitters using enzyme-based microelectrode arrays. In: *Electrochemical Methods for Neuroscience.* Michael A., (Ed), Francis Group LLC, Boca Raton, FL.

Hedou, C., Homberg, J., Martin, S., Wirth, K., Feldon, J. & Heidbreder, C.A. (2000) Effect of amphetamine on extracellular acetylcholine and monoamine levels in subterritories of the rat medial prefrontal cortex. *Eur. J. Pharmacol.*, **390**, 127–136.

Himmelheber, A.M., Sarter, M. & Bruno, J.P. (2000) Increases in cortical acetylcholine release during sustained attention performance in rats. *Brain Res. Cogn. Brain Res.*, **9**, 313–325.

Ibouz, N., Branski, L., Parnis, J., Parnas, H. & Linial, M. (1999) Depolarization affects the binding properties of muscarinic acetylcholine receptors and their interaction with proteins of the exocytotic apparatus. *J. Biol. Chem.*, **274**, 29519–29528.

Ichikawa, J., Dai, J., O'Laughlin, I.A., Fowler, W.L. & Meltzer, H.Y. (2002) Atypical, but not typical, antipsychotic drugs increase cortical acetylcholine release without an effect in the nucleus accumbens or striatum. *Neuropsychopharmacology*, **26**, 325–339.

Jones, B.E. (2005) From waking to sleeping: neuronal and chemical substrates. *Trends Pharmacol. Sci.*, **26**, 578–586.

Kennedy, R.T., Watson, C.J., Haskins, W.E., Powell, D.H. & Strecker, R.E. (2002) *In vivo* neurochemical monitoring by microdialysis and capillary separations. *Curr. Opin. Chem. Biol.*, **6**, 659–665.

Klein, J. (2000) Membrane breakdown in acute and chronic neurodegeneration: focus on choline-containing phospholipids. *J. Neural Transm.*, **107**, 1027–1063.

Klein, J., Koppen, A. & Loffelholz, K. (1991) Uptake and storage of choline by rat brain: influence of dietary choline supplementation. *J. Neurochem.*, **57**, 370–375.

Kozak, R., Bruno, J.P. & Sarter, M. (2006) Augmented prefrontal acetylcholine release during challenged attentional performance. *Cereb. Cortex*, **16**, 9–17.

Lowry, J.P., Miele, M., O'Neill, R.D., Boutelle, M.G. & Fillenz, M. (1998) An amperometric glucose-oxidase/poly (*o*-phenylenediamine) biosensor for monitoring brain glucose: *in vivo* characterization in the striatum of freely-moving rats. *J. Neurosci. Meth.*, **79**, 65–74.

Mechawar, N., Cozzari, C. & Descarries, L. (2000) Cholinergic innervation in adult rat cerebral cortex: a quantitative immunocytochemical description. *J. Comp. Neurol.*, **428**, 305–318.

Millan, M.J., Gobert, A., Roux, S., Porsolt, R., Meneses, A., Carli, M., Di Cara, B., Jaffard, R., Rivet, J.M., Lestage, P., Mocaer, E., Peglion, J.L. & Dekeyne, A. (2004) The serotonin1A receptor partial agonist S15535 [4-(benzodioxan-5-yl) 1-(indan-2-yl) piperazine] enhances cholinergic transmission and cognitive function in rodents: a combined neurochemical and behavioral analysis. *J. Pharmacol. Exp. Ther.*, **311**, 190–203.

Mitchell, K.M. (2004) Acetylcholine and choline amperometric enzyme sensors characterized *in vitro* and *in vivo*. *Anal. Chem.*, **76**, 1098–1106.

Nelson, C.L., Burk, J.A., Bruno, J.P. & Sarter, M. (2002) Effects of acute and repeated ketamine administration on cortical acetylcholine release and sustained attention. *Psychopharmacology*, **161**, 168–179.

Nelson, C.L., Sarter, M. & Bruno, J.P. (2000) Repeated pretreatment with amphetamine sensitizes increases in cortical acetylcholine release. *Psychopharmacology*, **151**, 406–415.

Parik, V. & Sarter, M. (2006) Cortical choline transporter function measured *in vivo* using choline-sensitive microelectrodes: clearance of endogenous and

exogenous choline and effects of removal of cholinergic terminals. *J. Neurochem.*, **97**, 488–503.
Parikh, V., Pomerleau, F., Huettl, P., Gerhardt, G.A., Sarter, M. & Bruno, J.P. (2004) Rapid assessment of *in vivo* cholinergic transmission by amperometric detection of changes in extracellular choline levels. *Eur. J. Neurosci.*, **20**, 1545–1554.
Passetti, F., Dalley, J.W., O'Connell, M.T., Everitt, B.J. & Robbins, T.W. (2000) Increased acetylcholine release in the rat medial prefrontal cortex during performance of a visual attention task. *Eur. J. Neurosci.*, **12**, 3051–3058.
Paxinos, G. & Watson, C. (1998) *The Rat in Stereotaxic Coordinates*. Academic Press, San Diego.
Phillips, P.E., Robinson, D.L., Stuber, G.D., Carelli, R.M. & Wightman, R.M. (2003) Real-time measurements of phasic changes in extracellular dopamine concentration in freely moving rats by fast-sacnning cyclic voltammetry. *Meth. Mol. Med.*, **79**, 443–464.
Pomerleau, F., Day, B.K., Huettl, P., Burmeister, J.J. & Gerhardt, G.A. (2003) Real time *in vivo* measures of L-glutamate in the rat central nervous system using ceramic-based multisite microelectrode arrays. *Ann. N.Y. Acad. Sci.*, **1003**, 454–457.
Richardson, N.R. & Gratton, A. (1998) Changes in medial prefrontal cortical dopamine levels associated with response-contingent food reward: an electrochemical study in rat. *J. Neurosci.*, **18**, 9130–9138.
Sarter, M. & Bruno, J.P. (1997) Cognitive functions of cortical acetylcholine: toward a unifying hypothesis. *Brain Res. Brain Res. Rev.*, **23**, 28–46.
Sarter, M., Givens, B. & Bruno, J.P. (2003) Attentional functions of cortical cholinergic inputs: What does it mean for learning and memory? *Neurobiol. Learn Mem.*, **80**, 245–256.
Sarter, M., Hasselmo, M.E., Bruno, J.P. & Givens, B. (2005) Unraveling the attentional functions of cortical cholinergic inputs: interactions between signal-driven and cognitive modulation of signal detection. *Brain Res. Rev.*, **48**, 98–111.
Szymusiak, R. (1995) Magnocellular nuclei of the basal forebrain: substrates of sleep and arousal regulation. *Sleep*, **18**, 478–500.
Talauliker, P.M., Rutherford, E.C., Pomerleau, F., Huettl, P., Stephens, M.L., Nickell, J.R., Hastings, J.T., Stromberg, I. & Gerhardt, G.A. (2005) *Multisite microelectrode array studies of 1-glutamate dynamics in the rodent hippocampus.* Program no. 966.11, 2005 (Abstract) Viewer/Itinerary Planner. Society for Neuroscience, Washington. D.C. Online.
Westerink, B.H.C. & DeVries, J.B. (2001) A method to evaluate the diffusion rate of drugs from a microdialysis probe through brain tissue. *J. Neurosci. Meth.*, **109**, 53–58.
Zaborszky, L. (2002) The modular organization of brain systems: basal forebrain: the last frontier. *Prog. Brain Rev.*, **136**, 359–372.
Zeisel, S.H. (1981) Dietary choline: biochemistry, physiology, and pharmacology. *Ann. Rev. Nutr.*, **1**, 95–121.